AJNR

This information is current as of July 24, 2025.

Effects of Arterial Stiffness on Cerebral WM Integrity in Older Adults: A Neurite Orientation Dispersion and Density Imaging and Magnetization Transfer Saturation Imaging Study

J. Kikuta, K. Kamagata, M. Abe, C. Andica, Y. Saito, K. Takabayashi, W. Uchida, H. Naito, H. Tabata, A. Wada, Y. Tamura, R. Kawamori, H. Watada and S. Aoki

Effects of Arterial Stiffness on Cerebral WM Integrity in Older Adults: A Neurite Orientation Dispersion and Density Imaging and Magnetization Transfer Saturation Imaging Study

J. Kikuta, K. Kamagata, M. Abe, C. Andica, Y. Saito, K. Takabayashi, W. Uchida, H. Naito, H. Tabata, A. Wada, Y. Tamura, R. Kawamori, H. Watada, and S. Aoki

ABSTRACT

BACKGROUND AND PURPOSE: Arterial stiffness is reported to be able to cause axonal demyelination or degeneration. The present study aimed to use advanced MR imaging techniques to examine the effect of arterial stiffness on the WM microstructure among older adults.

MATERIALS AND METHODS: Arterial stiffness was measured using the cardio-ankle vascular elasticity index (CAVI). The high-CAVI (mean CAVI $\geq$ 9 points) and the low-CAVI groups (mean CAVI $<$ 9 points) were created. The neuronal fiber integrity of the WM was evaluated by neurite orientation dispersion and density imaging and magnetization transfer saturation imaging. Tract-Based Spatial Statistics and the tracts-of-interest analysis were performed. Specific WM regions (corpus callosum, internal capsule, anterior thalamic radiation, corona radiata, superior longitudinal fasciculus, forceps minor, and inferior fronto-occipital fasciculus) were selected in the tracts-of-interest analysis.

RESULTS: In Tract-Based Spatial Statistics, the high-CAVI group showed a significantly lower myelin volume fraction value in the broad WM and significantly higher radial diffusivity and isotropic volume fraction values in the corpus callosum, forceps minor, inferior fronto-occipital fasciculus, internal capsule, corona radiata, and anterior thalamic radiation than the low-CAVI group. In tracts-of-interest analysis using multivariate linear regression, significant associations were found between the mean CAVI and radial diffusivity in the anterior thalamic radiation and the corona radiata; isotropic volume fraction in the anterior thalamic radiation and the corona radiata; and myelin volume fraction in the superior longitudinal fasciculus ($P < .05$). Additionally, partial correlation coefficients were observed for the significant associations of executive function with radial diffusivity and myelin volume fraction ($P < .05$).

CONCLUSIONS: Arterial stiffness could be associated with demyelination rather than axonal degeneration.

ABBREVIATIONS: ATR = anterior thalamic radiation; CAVI = cardio-ankle vascular elasticity index; CC = corpus callosum; CR = corona radiata; FA = fractional anisotropy; FMi = forceps minor; IC = internal capsule; IFOF = inferior fronto-occipital fasciculus; ISOVF = isotropic volume fraction; NODDI = neurite orientation dispersion and density imaging; MT = magnetization transfer; MVF = myelin volume fraction; RD = radial diffusivity; SLF = superior longitudinal fasciculus; TBSS = Tract-Based Spatial Statistics; TMT = Trail-Making Test; TOI = tracts of interest

Arterial stiffness can be measured by several different methods. The pulse wave velocity has been measured by various methods

as an indirect index of arterial elasticity, but it is blood pressure–dependent.[1] Conversely, the cardio-ankle vascular elasticity index (CAVI) directly reflects vascular elasticity and is blood pressure–independent.[2] Reports regarding the association between CAVI-measured arterial stiffness and WM microstructure have still not been published, though some studies reported the association between pulse wave velocity–measured arterial stiffness and brain WM integrity.

Neurite orientation dispersion and density imaging (NODDI) is a new, advanced DWI technique that improves WM characterization using a multicompartment model to describe different WM functions. By enabling the estimation of neurite structure, NODDI can provide more specific insight into the underlying WM microstructural changes.[3] Thus, NODDI could be useful in assessing arterial stiffness–associated WM microstructure, though no study has tested

Table 1: Demographic characteristics of the participants[a]

	All Participants (n = 110)	High-CAVI (n = 60)	Low-CAVI (n = 50)	High- vs Low-CAVI (P Value)
Sex (men/female)	66:44	37:23	29:21	.70
Age (yr)	72.65 (SD, 4.90)	72.72 (SD, 5.00)	72.58 (SD, 4.82)	.96
Mean CAVI	9.12 (SD, 0.84)	9.71 (SD, 0.57)	8.41 (SD, 0.46)	<.001
Antihypertensive therapy	71	43	28	.09
Education (yr)	14.31 (SD, 2.11)	14.30 (SD, 2.09)	14.32 (SD, 2.15)	.96
Body mass index	22.54 (SD, 2.84)	22.79 (SD, 2.54)	22.24 (SD, 3.16)	.31
Systolic blood pressure	137.47 (SD, 15.67)	139.60 (SD, 15.21)	134.92 (SD, 16.00)	.12
Diastolic blood pressure	86.05 (SD, 9.35)	86.52 (SD, 8.49)	85.48 (SD, 10.34)	.56
Heart rate	65.70 (SD, 23.73)	66.16 (SD, 33.88)	65.31 (SD, 9.85)	.85
Montreal Cognitive Assessment (Japanese version)	25.19 (SD, 2.87)	25.31 (SD, 2.95)	25.04 (SD, 2.66)	.61
Mini-Mental State Examination	27.93 (SD, 1.68)	28.07 (SD, 1.59)	27.76 (SD, 1.78)	.34
TMT A	42.51 (SD, 13.90)	43.32 (SD, 14.24)	41.54 (SD, 13.56)	.51
TMT B	115.82 (SD, 50.38)	116.78 (SD, 40.22)	114.66 (SD, 60.80)	.83
TMT B minus A	73.31 (SD, 44.11)	73.47 (SD, 36.01)	73.12 (SD, 52.60)	.97
Periventricular hyperintensity	1.14 (SD, 0.39)	1.17 (SD, 0.42)	1.10 (SD, 0.36)	.372
Deep and subcortical WM hyperintensity	1.25 (SD, 0.53)	1.31 (SD, 0.60)	1.18 (SD, 0.48)	.135

[a] Data are means.

this hypothesis. Moreover, myelin-sensitive imaging using MR imaging can evaluate the WM microstructure from a different viewpoint from DWI.

Arterial stiffness is indicated to cause axonal demyelination or degeneration.[4,5] Notably, Badji et al[6] showed that carotid-femoral pulse wave velocity is significantly associated with both fractional anisotropy (FA) and radial diffusivity (RD) but not with the myelin volume fraction (MVF). The results suggested that arterial stiffness is associated with axonal degeneration rather than with demyelination. However, reports supporting such results are still limited. We hypothesized that the impact of arterial stiffness on the brain WM microstructure could be better understood by using the above-mentioned multimodal WM-sensitive MR imaging techniques. Hence, this study aimed to explore the associations between CAVI-measured arterial stiffness and WM-sensitive MR imaging measures of the brain in older adults.

MATERIALS AND METHODS

The institutional review board of Juntendo University Hospital in Japan approved this study in compliance with the World Medical Association's Code of Ethics (Declaration of Helsinki) for experiments involving humans.

Study Participants

The Bunkyo Health Study is a prospective cohort study of 1629 older individuals.[7] Of these, 160 participants underwent both FLAIR imaging and DWI. Exclusion criteria included major psychiatric or neurologic disorders, heart failure, stroke, and/or a history of alcohol or drug abuse. Ultimately, 110 older participants were included for the analysis. Arteriosclerosis was estimated by CAVI determined by using an automatic waveform analyzer (Vascular Screening System VaSera VS1500; Fukuda Denshi).[8] High CAVI (≥9.0) implies progression of carotid and coronary arteriosclerosis;[9] thus, CAVI 9 was set as the cutoff value. The eligible participants were divided into the high-CAVI group (those with a mean [average of left and right values] CAVI of ≥ 9 points; 37 men and 23 women; mean age, 72.72 [SD, 5.00] years) and the

low-CAVI group (those with a mean CAVI of < 9 points; 29 men and 21 women; mean age, 72.58 [SD, 4.82] years). Table 1 shows the demographic characteristics. Deep and subcortical WM hyperintensity and periventricular hyperintensity were evaluated using the Fazekas scale,[10] according to axial FLAIR imaging.

Image Acquisition

MR imaging data were acquired using a 3T MR imaging scanner (Magnetom Prisma; Siemens) with a 64-channel head coil. We acquired multishell DWI data using a spin-echo echo-planar imaging sequence, which included 2 b-values of 1000 and 2000 s/mm^2 along 64 isotropic diffusion gradients uniformly distributed on a sphere, with a simultaneous multisection echo-planar imaging sequence in the anterior-posterior phase-encoding direction with the following parameters: TR = 3300 ms; TE = 70 ms; FOV = 229 × 229 mm; matrix size = 130 × 130; section thickness = 1.8 mm; resolution = 1.8 × 1.8 mm; acquisition time = 7 minutes and 29 seconds. DWI acquisition was completed with a b = 0 image. Standard and antiphase-encoded blipping images were acquired without diffusion weighting to compensate for the distortion caused by the magnetic susceptibility associated with the echo-planar imaging acquisition. The predominant T1-weighted, proton density–weighted, and magnetization transfer (MT)–weighted images were obtained using a 3D multiecho high-speed low-angle shot sequence for calculating the MT saturation index.[11] The settings for the MT saturation sequences were as follows: for MT$_{off}$ and MT$_{on}$ scanning, TE = 2.53 ms, TR = 24 ms, flip angle = 5°; for T1WI, TE = 2.53 ms, TR = 10 ms, flip angle = 13°, with parallel imaging using generalized autocalibrating partially parallel acquisition with a factor of 2 in the phase-encoding direction, 7/8 partial Fourier acquisition in the partition direction, bandwidth = 260 Hz/pixel, matrix = 128 × 128, acquisition time = 6 minutes 25 seconds, section thickness = 1.8 mm, FOV = 224 × 224 mm.

Diffusion MR Imaging Processing

For eliminating artifacts, the eddy (https://fsl.fmrib.ox.ac.uk/fsl/fslwiki/eddy/UsersGuide) and topup (https://fsl.fmrib.ox.ac.uk/

Table 2: Summary of WM metrics

Diffusion MR Imaging	Parameter	Explanation
DTI	FA	Overall direction of water diffusion in brain tissue
	Mean diffusivity	The magnitude of isotropic diffusion in brain tissue
	Axial diffusivity	The coefficient of diffusion across the long axis of the ellipsoid
	RD	The coefficient of diffusion perpendicular to the long axis
NODDI	Intracellular volume fraction	Neurite density based on intracellular diffusion
	Orientation dispersion index	Dispersion of neurites in the intracellular compartment
	ISOVF	The measure of extracellular water diffusion

fsl/fslwiki/topup) toolboxes, which are part of the FSL (www.fmrib.ox.ac.uk/fsl), were used.[12] The resulting images were fitted to the NODDI model[3] using the NODDI Matlab Toolbox 5 (http://www.nitrc.org/projects/noddi_toolbox). Table 2 summarizes the parameters of DTI and NODDI. The maps of the orientation dispersion index, isotropic volume fraction (ISOVF), and intracellular volume fraction were generated using the Accelerated Microstructure Imaging via Convex Optimization.[13] Furthermore, the DTIFit tool (https://open.win.ox.ac.uk/pages/fsl/fslpy/fsl.data.dtifit.html) was used to generate tensor-derived maps according to the ordinary least-squares method[14] using DWI data with b-values of 0 and 1000 s/mm^2.

Myelin-Sensitive Imaging Processing

MT saturation (MT$_{sat}$) data were analyzed using a Matlab script (https://www.mathworks.com/help/matlab/ref/run.html).[15] First, the apparent longitudinal relaxation rate (R_{1app}) was calculated as the following equation:

$$R_{1app} = \frac{1}{2} \frac{S_{T1}\alpha_{T1}/TR_{T1} - S_{PD}\alpha_{PD}/TR_{PD}}{S_{PD}/\alpha_{PD} - S_{T1}/\alpha_{T1}}.$$

Here, S_{T1} and S_{PD} indicate the signal strength of T1- and proton-density (PD)-weighted imaging, respectively. TR_{T1} and TR_{PD} reflect the TRs of T1- and PD-weighted imaging, respectively. α_{T1} and α_{PD} show the excitation flip angles of T1- and PD-weighted imaging. Second, the apparent signal amplitude (A_{app}) was calculated as the following:

$$A_{app} = S_{PD}S_{T1} \frac{TR_{PD}\alpha_{T1}/\alpha_{PD} - TR_{T1}\alpha_{PD}/\alpha_{T1}}{S_{T1}\ TR\alpha_{T1} - S_{PD}TR_{T1}\alpha_{PD}}.$$

Third, the apparent δ_{app} was calculated as the following equation:

$$\delta_{app} = (A_{app}\alpha_{MT}/S_{MT} - 1)R_{1app}TR_{MT} - \alpha_{MT}2/2.$$

TR_{MT}, S_{MT}, and α_{MT} show the TR, signal intensity, and excitation flip angle of the MT-weighted imaging respectively. The following formula was applied to fix the small residual high-order dependency of MT$_{sat}$ on the local radiofrequency (RF) transmit field:[16]

$$MT_{sat} = \frac{\delta_{app}(1 - 0.4)}{1 - 0.4\ RF_{local}}.$$

RF_{local} was calculated using the dual-angle method.[17] In addition, we added 2 B$_1$ maps with flip angles of 10° and 20°, respectively, obtained by echo-planar imaging in about 10 seconds. The first and second images were obtained after excitation with flip angles α and

2α proportional to sinα and sin 2α, respectively. The ratio of the 2 acquisitions was calculated using the following formula:

$$\frac{sin\alpha}{sin2\alpha} = \frac{1}{2cos\alpha}.$$

From there, the local flip angle α was calculated.

Tract-Based Spatial Statistics Analysis

Voxelwise statistical analysis was performed using Tract-Based Spatial Statistics (TBSS; http://fsl.fmrib.ox.ac.uk/fsl/fslwiki/TBSS) implemented in FSL.[18] The TBSS procedure was as follows: First, using FMRIB's Nonlinear Registration Tool (FNIRT; http://fsl.fmrib.ox.ac.uk/fsl/fslwiki/FNIRT), we aligned the FA maps of all participants into the Montreal Neurological Institute 152 standard space with $1 \times 1 \times 1$ mm^3 voxel size. Second, we created and thinned a population-based mean FA image to establish the mean FA skeleton, which shows the centers of all tracts common to the group. The threshold of the mean FA skeleton was 0.2 to exclude the peripheral tracts and GM. Third, a binary mask of the FA skeletonized image was used as the mask image to make a voxel-by-voxel statistical comparison between the high- and low-CAVI groups of the 4D skeleton image file. This comparison was performed using FSL's Randomise tool (http://fsl.fmrib.ox.ac.uk/fsl/fslwiki/Randomise/UserGuide), and the number of permutations was set to 10,000. The data for other WM metrics was analyzed using the tbss_non_FA script (https://fsl.fmrib.ox.ac.uk/fsl/fslwiki/TBSS/UserGuide#Using_non-FA_Images_in_TBSS) to generate a 4D skeleton image file for each metric.

Tract-of-Interest Analysis

Tracts of interest (TOI) were analyzed using the ICBM DTI-81 Atlas (http://www.bmap.ucla.edu/portfolio/atlases/ICBM_DTI-81_Atlas/).[19] According to the TBSS results (Figure) and previous studies showing arterial stiffness–associated WM regions, 6 major WM tracts, namely, the corpus callosum (CC), internal capsule (IC), corona radiata (CR), inferior fronto-occipital fasciculus (IFOF), forceps minor (FMi), and anterior thalamic radiation (ATR), were identified as TOI of RD and ISOVF. Additionally, 7 major WM tracts, namely, the CC, IC, CR, IFOF, FMi, ATR, and superior longitudinal fasciculus (SLF), were selected as TOI of the MVF. These WM regions are reportedly vulnerable to increased arterial stiffness.[4,5,20,21] Then, the mean value (the average of left and right values) within each ROI was computed for each WM metric.

Statistical Analysis

All statistical data were analyzed using SPSS Statistics, Version 27 (IBM). Demographic and clinical data were analyzed using the
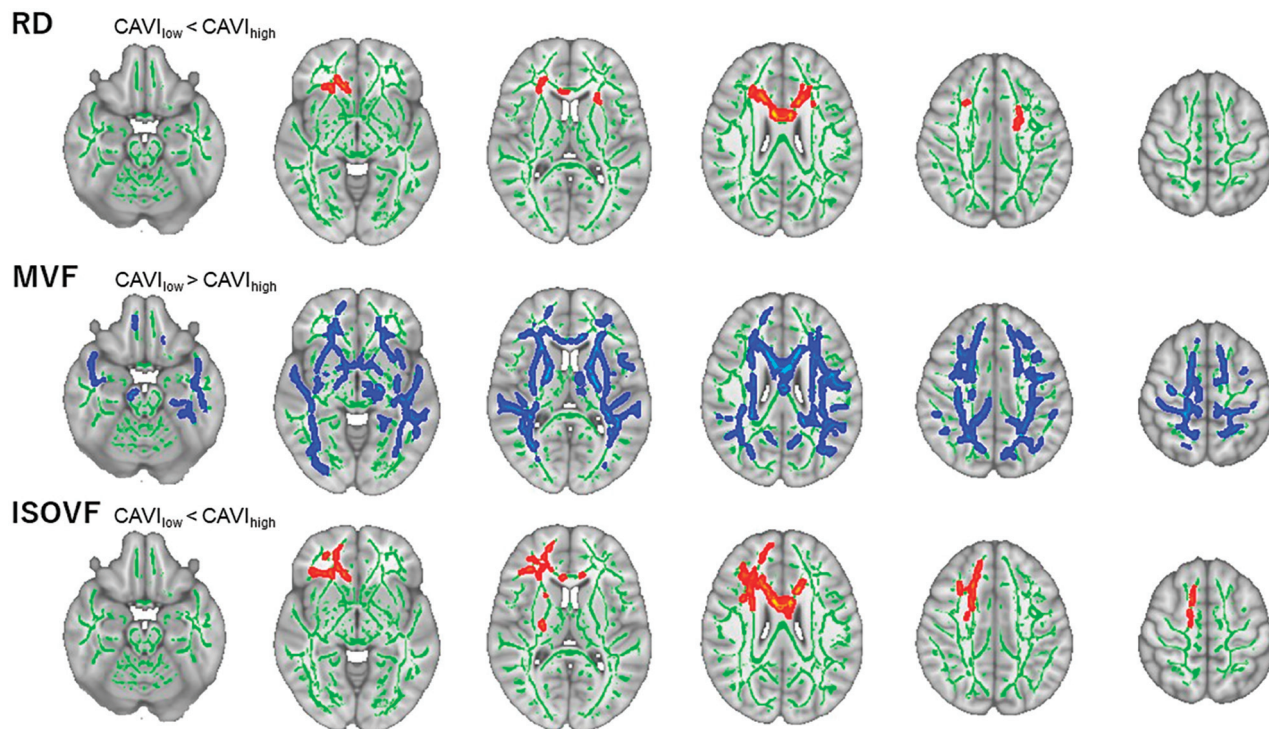
FIGURE. Comparison between the high- and low-CAVI groups. For TBSS, the low- and high-CAVI groups were compared (family-wise error–corrected $P < .05$, adjusting for age, sex, antihypertensive therapy use, intracranial volume, and systolic blood pressure). *Red–yellow voxels* demonstrate significantly higher RD and ISOVF values in the high-CAVI group than in the low-CAVI group. *Blue–light blue voxels* illustrate a significantly lower MVF value in the high-CAVI group than in the low-CAVI group.

χ^2 or Mann-Whitney U test. A P value (2-tailed) $< .05$ was considered statistically significant.

For TBSS, the high- and low-CAVI groups were compared using the Randomize tool (family-wise error–corrected $P < .05$, adjusting for age, sex, antihypertensive therapy use, systolic blood pressure, and intracranial volume).

In all participants, we applied univariate linear regression analyses for each WM metric as a dependent variable and the mean CAVI as an independent variable. Subsequently, multivariate linear regression analyses were conducted using backward linear regression to identify independent factors associated with the mean CAVI. The variable $P < .2$ in the univariate model was included in the back-removal procedure with P-removal $= .1$. Age, sex, antihypertensive therapy, systolic blood pressure, and intracranial volume were considered confounding covariates to separate from the strength of the relation between the mean CAVI and WM integrity.

Additionally, the partial correlation analyses between each WM metric and the cognitive performance scores were examined separately for all participants, the high-CAVI group, and the low-CAVI group, adjusting for age, sex, and education level. Multiple comparisons were corrected using the false discovery rate procedure for each WM metric and region.[22] The false discovery rate–corrected $P < .05$ was considered significant.

RESULTS

Participant Characteristics

Table 1 shows all participant characteristics. The high-CAVI group showed a significantly higher mean CAVI than the low-CAVI group. However, age, sex, education level, body mass index, heart rate, systolic blood pressure, diastolic blood pressure, and antihypertensive therapy history; the Mini-Mental State Examination; the Montreal Cognitive Assessment (Japanese version); Trail Making Test (TMT) A, TMT B, TMT B minus A; deep and subcortical WM hyperintensity; and periventricular hyperintensity were not significantly different between the 2 groups.

Whole-Brain Analysis

TBSS results identified a significantly lower MVF in the high-CAVI group than in the low-CAVI group in the broad WM area (family-wise error–corrected $P < .05$; Figure). RD was significantly higher in the high-CAVI group in specific WM areas such as the CC, FMi, bilateral IFOF, bilateral ATR, bilateral CR, and left IC compared with the low-CAVI group. The ISOVF was significantly higher in the high-CAVI group than in the low-CAVI group in the CC, FMi, right IC, right CR, right ATR, and right IFOF. Most interesting, RD and ISOVF changes were relatively overlapped, mainly observed in the anterior area. Whereas FA, mean diffusivity, axial diffusivity, the orientation dispersion index, and intracellular volume fraction did not significantly differ between 2 groups.

Tract-Specific Analysis

The univariate linear regression analysis revealed the significant associations of the mean CAVI with RD in the FMi; ISOVF in the CC, CR, and FMi; and MVF in the CR, IC, FMi, IFOF, ATR, and SLF (false discovery rate–corrected $P < .05$; Table 3). In the multivariate linear regression analyses adjusted for age, sex,

Table 3: Univariate and multivariate linear regression analyses adjusted for age, sex, anti-hypertensive therapy, systolic blood pressure, and intracranial volume for the association of mean CAVI with WM metrics in specific regions

	Univariate Linear Regression		Multivariate Linear Regression	
	P	β	P	β
RD				
ATR	.121	0.149	.015	1.549
CC	.075	0.171		
CR	.079	0.168	.004	−0.737
FMi	.01	0.245	.061	0.296
IC	.279	0.104		
IFOF	.163	0.134		
ISOVF				
ATR	.16	0.135	.014	−1.531
CC	.036	0.2		
CR	.031	0.206	.005	0.596
FMi	.037	0.2		
IC	.271	0.106		
IFOF	.123	0.148		
MVF				
ATR	.005	−0.265		
CC	.174	−0.13		
CR	.015	−0.231		
FMi	.028	−0.21		
IC	.009	−0.249		
IFOF	.019	−0.224		
SLF	.015	−0.231	.036	−0.218

Table 4: Partial correlation coefficients between WM metrics and TMT B, adjusted for age, sex, and education[a]

	All Participants		High-CAVI Group		Low-CAVI Group	
	Corrected P Value	r	Corrected P Value	r	Corrected P Value	r
RD						
ATR	.818	0.023	.898	−0.017	.545	0.090
CC	.121	0.160	.658	0.078	.291	0.174
CR	.046	0.220	.658	0.080	.107	0.307
FMi	.016	0.288	.650	0.135	.013	0.436
IC	.046	0.221	.650	0.152	.276	0.197
IFOF	.050	0.206	.650	0.121	.246	0.228
ISOVF						
ATR	.866	−0.016	.983	−0.008	.865	0.025
CC	.669	0.094	.983	0.003	.437	0.183
CR	.464	0.139	.983	0.055	.272	0.250
FMi	.464	0.147	.983	0.044	.256	0.297
IC	.822	0.059	.983	0.058	.865	0.047
IFOF	.861	−0.035	.983	−0.108	.788	0.095
MVF						
ATR	.042	−0.200	.549	−0.116	.054	−0.283
CC	.042	−0.200	.659	−0.060	.051	−0.324
CR	.022	−0.275	.549	−0.145	.027	−0.414
FMi	.026	−0.235	.614	−0.086	.051	−0.306
IC	.033	−0.219	.549	−0.134	.054	−0.283
ISOF	.022	−0.250	.549	−0.121	.051	−0.331
SLF	.022	−0.250	.549	−0.205	.051	−0.312

[a] False discovery rate–corrected P value <.05.

antihypertensive therapy, systolic blood pressure, and intracranial volume, the mean CAVI was significantly associated with RD and ISOVF in the ATR and CR, and the MVF in the SLF (false discovery rate–corrected $P < .05$; Table 3).

In all participants, the partial correlation analyses demonstrated significant associations of TMT B with RD in the CR, FMi, and IC, or MVF in all tested WM regions (false discovery rate–corrected $P < .05$; Table 4). In the low-CAVI group, TMT B was significantly associated with RD in the FMi and MVF in the CR (false discovery rate–corrected $P < .05$; Table 4). Furthermore, the partial correlation coefficients for the significant associations of TMT B minus A with RD in the CR, IC, and FMi and with MVF in the ATR, CR, and FMi were noted in all participants (false discovery rate–corrected $P < .05$; Table 5). Meanwhile, the low-CAVI group had partial correlation coefficients for the significant associations of TMT B minus A with MVF in the CC, CR, FMi, IC, IFOF, and SLF (false discovery rate–corrected $P < .05$; Table 5). However, the partial correlation coefficients showed no significant associations among the Mini-Mental State Examination, the Montreal Cognitive Assessment (Japanese version), and TMT A and WM metrics.

DISCUSSION

The present study evaluated the WM microstructural changes in older adults with arterial stiffness. The major findings are as follows: First, whole-brain voxelwise results identified a significantly lower MVF in the high-CAVI group than in the low-CAVI group in the broad WM regions. TBSS results also showed significantly higher RD and ISOVF in the high-CAVI group than in the low-CAVI group in the CC, FMi, IFOF, IC, CR, and ATR. Second, the multivariate linear analysis noted significant associations of the mean CAVI with RD and ISOVF in the ATR and CR; and with MVF in the SLF. Finally, we found partial correlation coefficients for the significant associations between the executive function scores and RD and MVF in specific WM areas.

Whole-brain voxelwise results revealed that the high-CAVI group had a significantly lower MVF value than the low-CAVI group in the broad WM area. Low MVF values indicate the loss of the myelin sheath insulating the nerves, implying WM demyelination.[23] In this study, the high-CAVI group also had higher RD and ISOVF values than the low-CAVI

Table 5: Partial correlation coefficients between WM metrics and TMT B minus A, adjusted for age, sex, and education[a]

	All Participants		High-CAVI Group		Low-CAVI Group	
	Corrected P Value	r	Corrected P Value	r	Corrected P Value	r
RD						
ATR	.286	0.104	.280	0.172	.846	0.029
CC	.060	0.199	.270	0.191	.508	0.127
CR	.019	0.262	.270	0.200	.162	0.283
FMi	.006	0.315	.270	0.265	.143	0.329
IC	.046	0.219	.270	0.203	.508	0.120
IFOF	.136	0.154	.419	0.109	.508	0.164
ISOVF						
ATR	.506	0.065	.333	0.187	.774	−0.053
CC	.233	0.153	.344	0.156	.774	0.099
CR	.201	0.178	.333	0.178	.774	0.156
FMi	.120	0.225	.333	0.230	.774	0.176
IC	.395	0.095	.333	0.176	.774	−0.043
IFOF	.386	−0.110	.526	−0.102	.774	−0.051
MVF						
ATR	.038	−0.232	.817	−0.207	.082	−0.256
CC	.088	−0.166	.855	0.025	.017	−0.390
CR	.038	−0.265	.817	−0.114	.008	−0.460
FMi	.038	−0.232	.817	−0.074	.019	−0.363
IC	.057	−0.192	.817	−0.083	.037	−0.314
IFOF	.051	−0.211	.847	−0.048	.017	−0.388
SLF	.057	−0.191	0.817	−0.088	.019	−0.358

[a] False discovery rate–corrected P value <.05.

group. High ISOVF values associated with high CAVI suggest increased extracellular water diffusion and have been shown to be related to increased inflammatory activation or blood-brain barrier permeability.[24] Moreover, elevated RD is also associated with demyelination.[25] From these results, the WM in the high-CAVI group could involve demyelination more than in the low-CAVI group. Furthermore, there were no significant differences in the degree of WM hyperintensities between the high- and low-CAVI groups in this study. Considering that TBSS showed significant differences in RD, ISOVF, and MVF between the two groups, our results suggest that WM microstructural changes precede WM hyperintensities and brain atrophy. In support of our findings, prior studies have indicated that DTI metrics capture ultrastructural changes in WM before the onset of WM hyperintensities and brain atrophy.[26,27] Therefore, it is thought that there was no correlation between the degree of WM hyperintensities and WM metrics.

In the multivariate linear analyses, the mean CAVI was significantly associated with RD in the ATR, CR, and FMi; ISOVF in the ATR and CR; and MVF in the SLF. These findings could reflect arteriosclerosis relating to demyelination. In previous studies, the WM microstructure has been reported to be vulnerable to circulatory alterations and correlates with arterial stiffness.[4-6,20] Notably, Badji et al[6] showed that carotid-femoral pulse wave velocity was significantly associated with both FA and RD but not with MVF.[17] The present study indicated the significant associations between the mean CAVI and not only DTI and NODDI metrics but also MVF, possibly reflecting the progression of arteriosclerosis exacerbating demyelination. The conflicting results regarding MVF between this study and that of Badji et al might be caused by differences in the characteristics of the target cohort. For instance, in our study, the average value of the body mass index (22.54 [SD, 2.84] kg/m^2) in all

participants was lower than that in the study of Badji et al (26.1 ([SD, 4.23] kg/m^2). However, the average value of systolic blood pressure (137.47 [SD, 15.67] mm Hg) in our study was higher than that in the study of Badji et al (125.66 [SD, 11.65] mm Hg). Suzuki et al[24] showed that pathologic processes related to hypertension are associated with image differences, suggesting changes in WM axons. In addition, WM integrity is particularly vulnerable to obesity.[28] A higher body mass index is associated with lower FA in the FMi and CC.[29] Therefore, except for the degree of arterial stiffness, the difference in participants' physical characteristics may influence WM integrity. However, exact matching of these clinical findings is difficult. Additionally, our participants were all Japanese, whereas the participants of Badji et al were all Canadian; thus, racial differences may affect WM integrity.[30]

The present study also showed the existence of the partial correlation coefficients for the significant associations between the executive function and WM metrics. In all participants and the low-CAVI group, the MVF in several WM areas was negatively associated with the executive function. These findings suggest that executive dysfunction may be associated with demyelination. However, in the high-CAVI group of the study, there was no significant connection between WM metrics and TMT scores, which are measures of executive function. Furthermore, although there was no difference in the TMT scores between the high- and low-CAVI groups, we found significant differences in WM metrics between two groups. The findings imply that WM microstructural changes may have already occurred before the impairment of executive function.

This study has some limitations. First, it is based on data obtained from Japanese individuals living in the city; hence, bias in genetic factors and environmental factors, such as eating habits, may occur. Second, it was conducted in a single facility. Thus, multicenter and epidemiologic studies are needed to examine further these investigations.

CONCLUSIONS

Arterial stiffness could be strongly associated with demyelination rather than axonal degeneration.

Disclosure forms provided by the authors are available with the full text and PDF of this article at www.ajnr.org.

REFERENCES

1. Lim J, Pearman M, Park W, et al. **Interrelationships among various measures of central artery stiffness.** *Am J Hypertens* 2016;29:1024–28 CrossRef Medline

2. Matsushita K, Ding N, Kim ED, et al. **Cardio-ankle vascular index and cardiovascular disease: systematic review and meta-analysis of prospective and cross-sectional studies.** *J Clin Hypertens (Greenwich)* 2019;21:16–24 CrossRef Medline

3. Zhang H, Schneider T, Wheeler-Kingshott CA, et al. **NODDI: practical in vivo neurite orientation dispersion and density imaging of the human brain.** *NeuroImage* 2012;61:1000–16 CrossRef Medline

4. Maillard P, Mitchell GF, Himali JJ, et al. **Aortic stiffness, increased white matter free water, and altered microstructural integrity: a continuum of injury.** *Stroke* 2017;48:1567–73 CrossRef Medline

5. Tarumi T, de Jong DL, Zhu DC, et al. **Central artery stiffness, baroreflex sensitivity, and brain white matter neuronal fiber integrity in older adults.** *Neuroimage* 2015;110:162–70 CrossRef Medline

6. Badji A, Noriega de la Colina A, Karakuzu A, et al. **Arterial stiffness and white matter integrity in the elderly: a diffusion tensor and magnetization transfer imaging study.** *Neuroimage* 2019;186:577–85 CrossRef Medline

7. Someya Y, Tamura Y, Kaga H, et al. **Skeletal muscle function and need for long-term care of urban elderly people in Japan (the Bunkyo Health Study): a prospective cohort study.** *BMJ Open* 2019;9:e031584 CrossRef Medline

8. Shirai K, Utino J, Otsuka K, et al. **A novel blood pressure-independent arterial wall stiffness parameter: cardio-ankle vascular index (CAVI).** *J Atheroscler Thromb* 2006;13:101–07 CrossRef Medline

9. Izuhara M, Shioji K, Kadota S, et al. **Relationship of cardio-ankle vascular index (CAVI) to carotid and coronary arteriosclerosis.** *Circ J* 2008;72:1762–67 CrossRef Medline

10. Fazekas F, Chawluk JB, Alavi A, et al. **MR signal abnormalities at 1.5 T in Alzheimer's dementia and normal aging.** *AJR Am J Roentgenol* 1987;149:351–56 CrossRef Medline

11. Kamagata K, Zalesky A, Yokoyama K, et al. **MR g-ratio-weighted connectome analysis in patients with multiple sclerosis.** *Sci Rep* 2019;9:13522 CrossRef Medline

12. Yamada H, Abe O, Shizukuishi T, et al. **Efficacy of distortion correction on diffusion imaging: comparison of FSL Eddy and Eddy_Correct using 30 and 60 directions diffusion encoding.** *PLoS One* 2014;9:e112411 CrossRef Medline

13. Daducci A, Canales-Rodríguez EJ, Zhang H, et al. **Accelerated Microstructure Imaging via Convex Optimization (AMICO) from diffusion MRI data.** *Neuroimage* 2015;105:32–44 CrossRef Medline

14. Basser PJ, Mattiello J, LeBihan D. **Estimation of the effective self-diffusion tensor from the NMR spin echo.** *J Magn Reson B* 1994;103:247–54 CrossRef Medline

15. Helms G, Dathe H, Kallenberg K, et al. **High-resolution maps of magnetization transfer with inherent correction for RF inhomogeneity and T1 relaxation obtained from 3D FLASH MRI.** *Magn Reson Med* 2008;60:1396–407 CrossRef Medline

16. Weiskopf N, Suckling J, Williams G, et al. **Quantitative multi-parameter mapping of R1, PD*, MT, and R2* at 3T: a multi-center validation.** *Front Neurosci* 2013;7:95 CrossRef Medline

17. Morrell GR, Schabel MC. **An analysis of the accuracy of magnetic resonance flip angle measurement methods.** *Phys Med Biol* 2010;55:6157–74 CrossRef Medline

18. Smith SM, Jenkinson M, Johansen-Berg H, et al. **Tract-Based Spatial Statistics: voxelwise analysis of multi-subject diffusion data.** *Neuroimage* 2006;31:1487–505 CrossRef Medline

19. Mori S, Oishi K, Jiang H, et al. **Stereotaxic white matter atlas based on diffusion tensor imaging in an ICBM template.** *Neuroimage* 2008;40:570–82 CrossRef Medline

20. Maillard P, Mitchell GF, Himali JJ, et al. **Effects of arterial stiffness on brain integrity in young adults from the Framingham heart study.** *Stroke* 2016;47:1030–36 CrossRef Medline

21. Tamura Y, Shimoji K, Ishikawa J, et al. **Subclinical atherosclerosis, vascular risk factors, and white matter alterations in diffusion tensor imaging findings of older adults with cardiometabolic diseases.** *Front Aging Neurosci* 2021;13:712385 CrossRef Medline

22. Benjamini Y, Hochberg Y. **Controlling the false discovery rate: a practical and powerful approach to multiple testing.** *Journal of the Royal Statistical Society: Series B (Methodological)* 1995;57:289–300

23. Duval T, Stikov N, Cohen-Adad J. **Modeling white matter microstructure.** *Funct Neurol* 2016;31:217–28 CrossRef Medline

24. Suzuki H, Gao H, Bai W, et al. **Abnormal brain white matter microstructure is associated with both pre-hypertension and hypertension.** *PLoS One* 2017;12:e0187600 CrossRef Medline

25. Song SK, Yoshino J, Le TQ, et al. **Demyelination increases radial diffusivity in corpus callosum of mouse brain.** *Neuroimage* 2005;26:132–40 CrossRef Medline

26. Andica C, Kamagata K, Hatano T, et al. **Free-water imaging in white and gray matter in Parkinson's disease.** *Cells* 2019;8:839 CrossRef Medline

27. Maillard P, Carmichael O, Harvey D, et al. **FLAIR and diffusion MRI signals are independent predictors of white matter hyperintensities.** *AJNR Am J Neuroradiol* 2013;34:54–61 CrossRef Medline

28. Bettcher BM, Walsh CM, Watson C, et al. **Body mass and white matter integrity: the influence of vascular and inflammatory markers.** *PLoS One* 2013;8:e77741 CrossRef Medline

29. Kullmann S, Schweizer F, Veit R, et al. **Compromised white matter integrity in obesity.** *Obes Rev* 2015;16:273–81 CrossRef Medline

30. Liu G, Allen B, Lopez O, et al. **Racial differences in gray matter integrity by diffusion tensor in black and white octogenarians.** *Curr Alzheimer Res* 2015;12:648–54 CrossRef Medline